Computers and Geotechnics 63 (2015) 73–82

Contents lists available at ScienceDirect

Computers and Geotechnics

journal homepage: www.elsevier.com/locate/compgeo

Non-linear analysis of vertically loaded piled rafts

Francesco Basile *

Geomarc Ltd, Via G. Bruno 106, 98123 Messina, Italy

ARTICLE INFO

Article history:
Received 20 March 2014
Received in revised form 23 July 2014
Accepted 25 August 2014

Keywords:
CPRF
Piled raft
Pile group
Non-linear

ABSTRACT

While the availability of 3D FEM or FDM analyses has greatly contributed to the increasing use of piled rafts for high rise structures, there is a need in industry for practical analysis methods which would also allow the adoption of piled rafts for more ordinary structures. For this purpose, a 3D boundary element solution is proposed for computing the non-linear response of piled rafts to vertical loads. The validity of the analysis is demonstrated through comparison with alternative numerical solutions and field measurements. Examples are given to demonstrate the basic importance of considering soil nonlinearity effects in design, thereby leading to more realistic predictions of the raft and pile response. The key feature of the proposed approach lies in its computational efficiency which makes the analysis economically viable not only for the design of piled rafts supporting high rise buildings (generally based on complex and expensive 3D FEM or FDM analyses) but also for that of bridges, viaducts and normal buildings.

1. Introduction

In conventional foundation design, it is assumed that the applied load is carried either by the raft or by the piles, considering the safety factors in each case. In recent years, an increasing number of structures (especially tall buildings) have been founded on Combined Pile–Raft Foundations (CPRFs), an attractive foundation system which allows the load to be shared between the raft and the piles, thereby offering a more economical solution. In the design of piled rafts, a sufficient safety against geotechnical failure of the *overall* pile–raft system has to be achieved, while the piles may potentially be used up to their ultimate geotechnical capacity. Contrary to traditional pile foundation design, no proof for the ultimate capacity of each individual pile is necessary [14]. Given the high load level at which the piles operate, consideration of soil nonlinearity effects is essential, and ignoring this aspect can lead to inaccurate predictions of the deformations and structural actions within the system.

Due to the 3D nature of the problem and the complexity of soil-structure interaction effects, calculation procedures for piled rafts are based on numerical analyses, ranging from simplified Winkler approaches to rigorous 3D finite element (FEM) or finite difference (FDM) solutions using available packages. Winkler approaches employ a "plate on springs" model in which the raft is represented by a plate and the piles as springs (e.g. [7,25,15,19,22,13]). Although such approaches are attractive in their flexibility (e.g. enabling non-linear soil response to be incorporated easily), they suffer from some restrictions mainly related to their semi-empirical nature and fundamental limitations (e.g. disregard of soil continuity).

A more rational approach is offered by soil continuum-based solutions such those based on the boundary element method (BEM) in which both the raft and the piles within the system are discretized using elastic theory (e.g. [5,17]). Several hybrid approaches have also been developed, in which the raft is modelled via FEM and the piles are modelled either via BEM [11] or using the finite layer method [35]. All these analyses are however restricted to linear elastic soil behaviour.

The above restriction may be removed by using 3D FEM and FDM solutions (e.g. Plaxis 3D and FLAC-3D) which allow complex geometries and soil behaviour to be modelled, while retaining continuity within the soil mass. However, such analyses are burdened by the high computational cost and specialist expertise needed for their execution, particularly when non-linear soil behaviour is to be considered. Major difficulties are related to the high mesh dependency and the uncertainty in assigning mechanical properties to the pile–soil interface elements (e.g. [18]). This aspect restricts their practical application in routine design, where multiple load cases need to be examined and where the pile number, properties, and location may have to be altered several times in order to obtain an optimised solution. This is particularly true in the case of "ordinary" piled rafts (e.g. bridges, viaducts, wind turbines, normal buildings) where the cost and complexity of conducting 3D FEM or FDM analyses can rarely be justified.

In an attempt to provide a practical tool for the designer, the paper describes an efficient analysis method for computing the

* Tel.: +39 090 2939038; fax: +39 090 2926576.
E-mail address: francesco.basile@geomarc.it

http://dx.doi.org/10.1016/j.compgeo.2014.08.011
0266-352X/

response of piled rafts. The originality of the approach lies in its capability to provide a non-linear BEM solution of the soil continuum, while retaining a computationally efficient code, thereby removing some of the limitations of current design methods. The validity of the proposed analysis is assessed through a comparison with alternative numerical solutions and a published case history. Examples are given to highlight the significance of considering soil nonlinearity effects, thereby leading to more realistic predictions of the raft and pile response.

2. Analysis method

The safe and economic design of piled rafts requires non-linear methods of analysis which have the capacity of simulating all relevant interactions between the foundation elements and the subsoil, specifically (1) pile–soil-interaction (i.e. single pile response including shaft-base interaction), (2) pile–pile-interaction (i.e. group effects), (3) raft–soil-interaction, and (4) pile–raft interaction, as illustrated in Fig. 1a [14].

The proposed method is an extension to the raft analysis of the non-linear BEM formulation employed in the pile-group program PGROUPN [2] and widely used in pile design through the software Repute [3]. The main feature of the approach lies in its ability to perform a complete 3D BEM analysis of the soil continuum (i.e. the simultaneous influence of all the pile and raft elements is considered), while incurring negligible computational costs. Indeed, compared to 3D FEM or FDM analyses, BEM provides a complete problem solution in terms of boundary values only, specifically at the raft–pile–soil interface. This leads to a drastic reduction in unknowns to be solved, thereby resulting in substantial savings in computing time and data preparation effort. This feature is particularly significant for three-dimensional problems and makes the analysis economically viable not only for the design of piled rafts supporting high rise buildings (generally based on complex and expensive 3D FEM or FDM analyses) but also for that of bridges, viaducts and ordinary buildings.

The main capabilities of the PGROUPN program, including the proposed extension to the raft analysis, are summarised below:

- based on 3D complete BEM solution of the soil continuum;
- models all relevant interactions (i.e. pile–soil, pile–pile, raft–soil, and pile–raft);
- piles in any configuration and having different characteristics within the same group (e.g. stiffness, length, rake, shaft and base diameter);
- piles connected by fully rigid ground-contacting raft;
- non-homogeneous and layered soil profiles;
- linear or non-linear continuum-based soil model;
- general 3D loading conditions, including any combination of vertical, horizontal, moment, and torsional loading;
- output includes the distribution of displacements, stress, forces, and moments along the piles, plus the normal stress, displacements, and rotations of the pile cap.

2.1. PGROUPN boundary element formulation

A detailed description of the theoretical formulation adopted in PGROUPN for the case of pile groups has been presented elsewhere [1,2]. The boundary element modelling of the soil-structure interaction for the piles and for the raft is similar and, hence, only a brief outline of the raft analysis is given below. Similarly to the discretization of the pile–soil interface into a number of cylindrical elements, the approach is now extended to the raft analysis (including its reciprocal interaction with the piles) by discretizing the raft–soil interface into a number of rectangular elements (Fig. 1b). The behaviour of each element is considered at a node (located at the centre of the element), each element being acted upon by uniform normal stress. Thus, only the bearing contribution of the raft underside is considered (i.e. the raft–soil interface is assumed to be smooth). It should be emphasised that the analysis takes into account the simultaneous influence of all the raft and pile elements within the foundation system, i.e. a "complete" solution of the soil continuum is adopted. All four of the above interactions (i.e. pile–soil, pile–pile, raft–soil, and pile–raft) are therefore evaluated as a matter of course, thereby overcoming the approximations of the traditional interaction factor approach and the fundamental limitations of Winkler models (based on empirical multipliers to account for group action). In addition, by retaining soil continuity, the input soil parameters required by PGROUPN have a clear physical meaning (e.g. the soil Young's modulus and strength properties) and can be measured directly in a soil investigation. This aspect represents a significant advantage over Winkler approaches which disregard soil continuity and, therefore, have to rely on empirical parameters (e.g. the modulus of subgrade reaction).

The boundary element method involves the integration of an appropriate elementary singular solution for the soil medium over the surface of the problem domain, i.e. the raft–soil interface. Under the assumption of purely linear elastic soil behaviour, the well-established solution of Mindlin [20] is adopted to correlate soil stress (t_s) and displacements (u_s) at the raft–soil interface:

$$u_s = [G_s]t_s \tag{1}$$

where $[G_s]$ is the soil flexibility matrix obtained from Mindlin's solution. The singular part of the $[G_s]$ matrix is calculated via analytical integration of the Mindlin functions over each

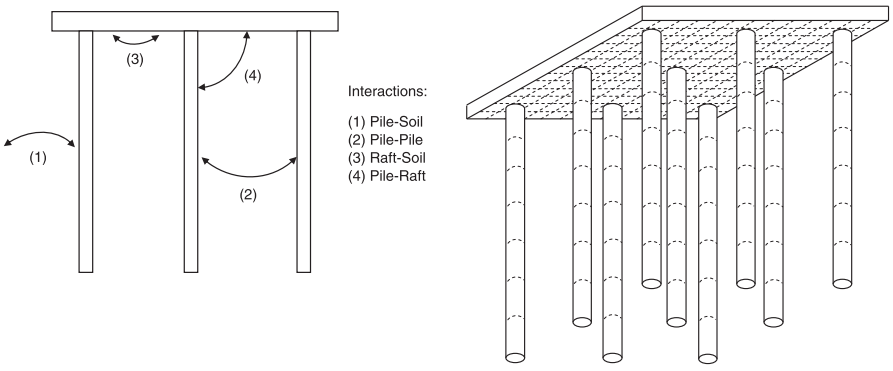

Fig. 1. (a) Soil-structure interactions in piled raft and (b) PGROUPN boundary element mesh.

rectangular element, therefore resulting in substantial savings in computing time. It is noted that Mindlin's solution is strictly applicable to homogeneous soil conditions. In practice, however, this limitation is not strictly adhered to, and non-homogeneous multi-layered soil profiles are often treated approximately using some averaging of the soil moduli [24]. Thus, in the evaluation of the soil modulus at the raft–soil interface elements, an equivalent value is calculated on the basis of weighted average values of soil modulus at each soil layer as proposed by Fraser and Wardle [10] and applied to this type of problems by Kitiyodom et al. [16]. The BEM formulation is generally based on a sub-structuring technique in which the raft and the surrounding soil are considered separately and then coupled. However, under the assumption of perfectly rigid (and elastic) raft, no corresponding equation for the raft flexibility is required and therefore Eq. (1) for the soil domain can be solved directly for the raft stress (t_c) by successively applying unit boundary conditions to the raft (i.e. unit vertical displacement and rotations), while enforcing the conditions of displacement compatibility ($u_s = u_c$, where u_c are the raft displacements) and stress equilibrium ($t_s = -t_c$) at the raft–soil interface. This leads to the system of vertical loads and moments acting on the raft that are necessary to equilibrate the raft contact stress. Thus, the external vertical load (V) and moments (M_{xz} and M_{yz}) acting on the cap can be related to the corresponding vertical displacement (w) and rotations (θ_{xz} and θ_{yz}) of the cap via:

$$\begin{Bmatrix} V \\ M_{xz} \\ M_{yz} \end{Bmatrix} = [K] \begin{Bmatrix} w \\ \theta_{xz} \\ \theta_{yz} \end{Bmatrix} \tag{2}$$

where the coefficients of the (3×3) $[K]$ matrix are the equilibrating forces as discussed above. The $[K]$ matrix can be regarded as the global stiffness matrix of the raft–soil system (which may be used as boundary conditions for the superstructure analysis). By inverting the $[K]$ matrix, the global flexibility matrix of the raft–soil system is obtained, and hence the vertical displacement and rotations of the pile cap may be derived for any loading condition. Finally, by scaling the raft stress due to unit boundary conditions using the cap displacement and rotations obtained from Eq. (2), the raft contact stress for the prescribed loading conditions is obtained.

It should be emphasised that any combination of vertical, horizontal, and moment loading can be applied to the piled raft. However, while the vertical and moment load is carried partly by the piles and partly by the raft contact pressures, the lateral load is entirely taken by the piles, given that only the bearing contribution of the raft underside is considered. Indeed, frictionless contact between raft and soil is assumed, so that no interfacial shear stresses are allowed to develop, which is a common assumption in design practice.

2.1.1. Limiting raft–soil stress

The foregoing procedure is based on the assumption that the soil behaviour is linear elastic. However, it is essential to ensure that the stress state at the raft–soil interface does not violate the yield criteria. This can be achieved by specifying limiting values of raft–soil contact pressure (based on the traditional bearing capacity theory) in order to allow for local bearing failure of the raft, while no tension is assumed to develop at the raft–soil interface. For cohesive soils, following a total stress approach, the limiting bearing stress (q_u) at the raft–soil interface may be expressed as [27,21]:

$$q_u = 6C_u \tag{3}$$

where Cu is the soil undrained shear strength. For cohesionless soils, following an effective stress approach, the limiting bearing stress at the raft–soil interface is taken as [21]:

$$q_u = 0.5\gamma' B N_\gamma + \sigma'_v N_q \tag{4}$$

where γ' is the effective unit weight, B is the raft width, σ'_v is the effective vertical stress, and N_γ and N_q are the bearing capacity factors as reported by Brinch Hansen [4].

2.1.2. Non-linear soil behaviour

Similarly to the pile analysis [2], non-linear soil behaviour is modelled, in an approximate manner, by assuming that the tangent soil Young's modulus (E_{tan}) varies with the raft–soil interface stress (t) according to the common hyperbolic stress–strain law [8,24]:

$$E_{tan} = E_i(1 - R_f t/t_{lim})^2 \tag{5}$$

where E_i is the initial soil modulus, R_f is the hyperbolic curve-fitting constant and t_{lim} is the limiting value of the raft–soil stress as specified in Eqs. (3) and (4). Thus, Eq. (1) is solved incrementally (under unit boundary conditions) using the modified values of the soil Young's modulus of Eq. (5) within the soil matrix $[G_s]$, while enforcing the conditions of yield, equilibrium and compatibility at the raft–soil interface. For the raft–soil interface elements which have yielded, no more increment in stress is permitted and any increase in load is therefore redistributed between the remaining elastic elements until all elements have failed. It is noted that yielding of an element introduces a discontinuity in the material property and, therefore, the use of Mindlin's solution to determine the remaining elastic coefficients is only approximate. However, previous work indicates that the errors engendered by this approach are slight (e.g. [24,1]).

The hyperbolic curve fitting constant R_f in Eq. (5) defines the degree of curvature of the stress–strain response and its value can range between 0 (an elastic-perfectly plastic response) and 0.99 ($R_f = 1$ is representative of an asymptotic hyperbolic response in which the limiting value of raft–soil stress is never reached). The most reliable method to determine the value of R_f is by back-fitting the PGROUPN load–settlement curve with the measured data from a loading test on a full-scale raft. In the absence of any test data, taking into account the high nonlinearity of response, the value of R_f can be taken as 0.9 based on the findings of Duncan and Chang.

2.2. Assumption of fully rigid raft

The PGROUPN analysis is currently restricted to the assumption of perfectly rigid raft. In practice, this assumption makes the analysis strictly applicable to "small" piled rafts [36], i.e. those rafts in which the bearing capacity of the unpiled raft is generally not sufficient to carry the applied load with a suitable safety margin, and hence the primary reason for adding piles is to increase the factor of safety. This typically involves rafts in which the width (B_r) amounts to a few meters (typically $5\ \text{m} < B_r < 15\ \text{m}$) and is small in comparison to the length (L) of the piles (i.e. $B_r/L < 1$). Within this range (whose limits should however be regarded as tentative and indicative only), the raft response may be considered as truly rigid and hence the design should aim at limiting the maximum settlement (being the differential settlements negligible). In practical applications, a simple check on the validity of the assumption of rigid raft may be performed by calculating the raft–soil stiffness ratio (K_{rs}) as defined by Horikoshi and Randolph [12]:

$$K_{rs} = 5.57 \frac{E_r}{E_s} \frac{1 - \nu_s^2}{1 - \nu_r^2} \left(\frac{B_r}{L_r}\right)^{0.5} \left(\frac{t_r}{L_r}\right)^3 \tag{6}$$

where the subscripts r and s denote the raft and soil properties, respectively, E is the Young's modulus, ν is the Poisson's ratio, B_r is the raft width, L_r is the raft length (with $B_r \leqslant L_r$), and t_r is the raft thickness. For values of $K_{rs} > 5$–10, the raft can be considered as rigid while a lower limit $K_{rs} > 1.5$ may be assumed for practical

purposes [29]. It is however observed that the above definition of K_{rs} does not include the additional stiffening contribution provided by the piles and by the superstructure which in effect increases the actual raft rigidity. Clearly, for "large" flexible rafts (in which typically $B_r/L > 1$ according to the definition by Viggiani and colleagues), the assumption of rigid raft is no longer valid and the limitation of differential settlement becomes one of the design requirements. However, except for thin rafts, the maximum settlement and the load sharing between the raft and the piles are little affected by the raft rigidity (e.g. [27,33]).

It should be emphasised that the current assumption of fully rigid raft prevents the application of PGROUPN to those piled rafts in which the raft flexibility plays a major role in design optimisation. Indeed, this includes determining the optimum combination of raft thickness and pile characteristics (number, layout, length, diameter) in order to achieve an economical and effective design. However, the proposed PGROUPN program can be useful in those situations where the piled raft is essentially designed as a pile group with a rigid cap (e.g. for a bridge pier), while making use of the extra raft component of capacity in order to reduce the piling requirements which are necessary to achieve the design criteria (e.g. bearing capacity, settlement). This type of piled raft can be regarded as a 'raft-enhanced pile group' (according to the definition of [23]), i.e. a pile group which has been value-engineered in order to take advantage of the raft contribution for resisting the applied loads. As discussed by O'Brien and colleagues, the design concept of 'raft-enhanced pile group' is different from that of conventional CPRF or 'pile-enhanced raft'. Indeed, in a pile-enhanced raft, the raft will usually carry the bulk of the design load, while the piles are added to resolve local non-compliances (e.g. differential settlements, raft shear force or bending moment). In such cases, it might not be necessary to take into account the piles' capacity component into the overall geotechnical bearing capacity. In contrast, in raft-enhanced pile groups, the piles usually attract most of the overall design load, and use is made of the extra raft capacity to reduce the piling requirements (in raft-enhanced pile groups, the raft typically takes between 20% and 50% of the total load).

3. Numerical results

The validity of the proposed analysis is verified through a comparison with alternative numerical solutions and a published case history.

3.1. Comparison with Kuwabara [17]

The accuracy of PGROUPN is initially assessed in the linear elastic range for the piled raft (3×3 group) sketched in Fig. 2. The figure shows the dimensionless load–settlement ratio (P/E_sDw, where P is the total applied load and w is the settlement) of the piled raft for a wide range of pile length-diameter ratios (L/D). For comparison, results from the corresponding free-standing pile group are also reported and show the small influence of the raft contribution to the resulting settlement, in line with current understanding. However, the load distribution is considerably affected by consideration of the ground-contacting raft, as illustrated in Fig. 3a which shows the percentage of the total load carried by the raft and by the corner pile as a function of the L/D ratio. The figure shows that the raft load decreases with increasing pile length, given that the longer the piles, the more load is taken by the piles. For comparison, the load taken by the corner pile of the pile group is also reported, showing a significant reduction of corner load in the piled raft as compared to the pile group.

Such reduction is also evident in Fig. 3b which compares the axial load profile $P(z)$ (where $P_{av} = P/9$ is the average pile head-load in the free-standing group) along the corner and the centre pile of the piled raft and the pile group (with $L/D = 25$). It is worth noting that the presence of the ground-contacting raft leads to an increase of axial load in the upper portion of the piles, particularly in the centre pile. This is a consequence of the additional vertical soil displacements caused by the ground-contacting raft, leading to a local downward movement of the soil relative to the pile. In this condition, the shear stress reverses sign (i.e. it becomes negative), thereby resulting in a local increase of axial load. Clearly, the above effect is more significant in the upper portion of the central pile, the most affected by raft–pile–soil interaction (due to the combined influence of raft–pile and pile–pile interaction effects). Overall, Figs. 2 and 3 show a favourable agreement of PGROUPN with the boundary element solution of Kuwabara [17], the variational approach of Shen et al. [31], and the hybrid analysis of Ta and Small [35] which combines the FEM for the raft with the finite layer method for the piles.

3.2. Comparison with Kitiyodom and Matsumoto [15]

A comparison is carried out for a square rigid raft supported by 2×2 piles and embedded in five different linear elastic soil profiles, as shown in Fig. 4 and described by Kitiyodom and Matsumoto [15]. The settlement of the piled raft and the percentage of total load ($V = 900$ kN) carried by the raft are reported in Fig. 5, showing a good agreement of PGROUPN with the two analyses carried out by Kityodom and Matsumoto, i.e. a rigorous 3D FEM solution and a "plate on springs" approach (incorporated in the program PRAB) in which the raft is modelled as a thin plate, the piles as elastic beams, the soil as springs, and use is made of Mindlin's solution to account for the interaction between structural members.

3.3. Comparison with Kitiyodom et al. [16]

Fig. 6 reports the normalised settlement (wE_s/qL_R) and the percentage of total load taken by the piles as a function of the pile length-diameter ratio (L/D) for a square rigid raft (having a width of L_R), supported by 8×8 piles at a spacing-diameter ratio $s/D = 6.25$, embedded in a deep homogeneous elastic soil layer (having a soil Young's modulus E_s), and subjected to an uniform vertical load (q), as reported by Kitiyodom et al. [16]. The figure shows a favourable agreement of PGROUPN with the analysis of Kitiyodom et al. [16] (using the program PRABS, a simplified version of the PRAB program described above in which each pile is now modelled by a single spring of equivalent stiffness), the program GARP by Poulos [25] (employing a "plate on springs" model), and the hybrid analysis of Hain and Lee [11] (which combines the FEM for the raft with a BEM-based interaction factor procedure to account for the interaction between structural members).

3.4. Comparison with Poulos [26,27]

Although the numerical results presented above are all based on the assumption of linear elastic soil behaviour (mainly due to the limitations of the numerical approaches used for comparison), it is essential to consider the effects of soil nonlinearity for a more realistic response. For this purpose, the piled raft (3×3 group) shown in Fig. 7 is examined, as reported by Poulos [26,27]. The raft bearing capacity is taken as 300 kPa with a pile load capacity of 873 kN in compression and 786 kN in tension. In order to compare PGROUPN results with those of alternative numerical analyses, three different soil models are employed: linear elastic (indicated as LE), non-linear (indicated as NL, using the following hyperbolic constants from Eq. (5): $R_f = 0.9$ for the raft and the standard values $R_f = 0.5$ for the pile shaft and $R_f = 0.99$ for the pile base, as reported in [2], and elastic-perfectly plastic (indicated as EP, adopting $R_f = 0$

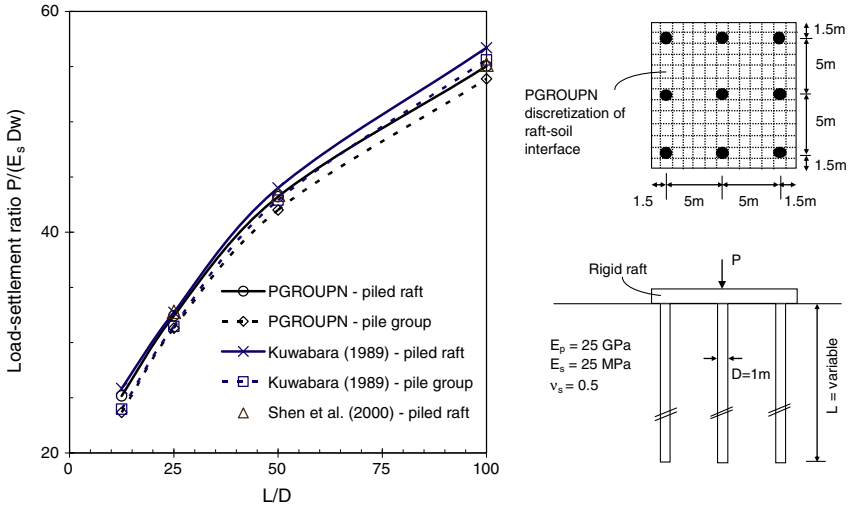

Fig. 2. Load–settlement ratio and piled raft analysed.

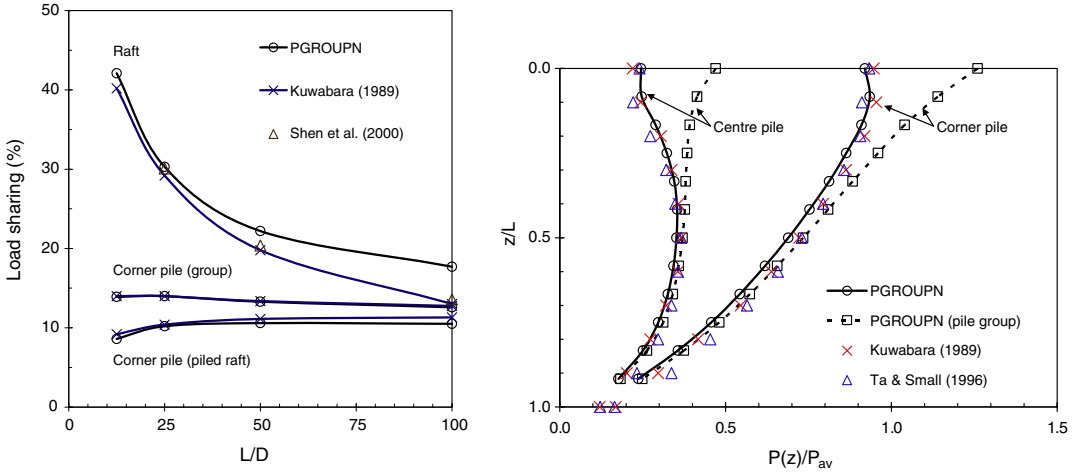

Fig. 3. (a) Load sharing between raft and piles and (b) axial distribution of pile load.

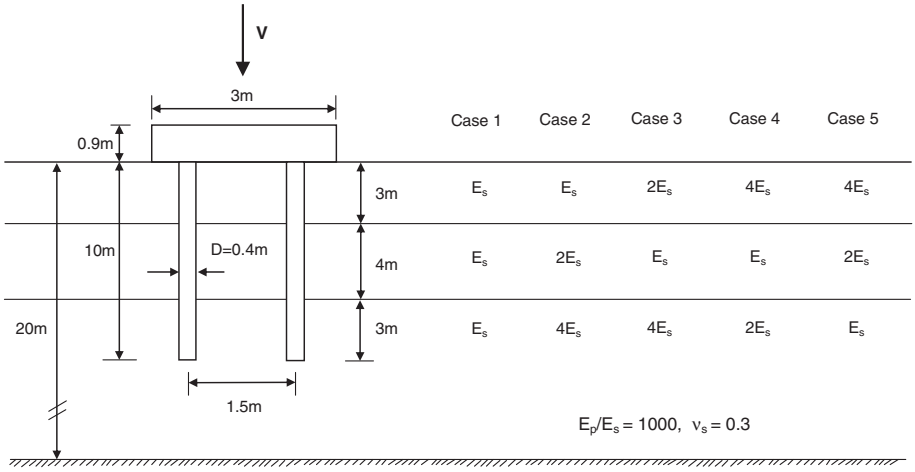

Fig. 4. Piled raft and soil profiles analysed.

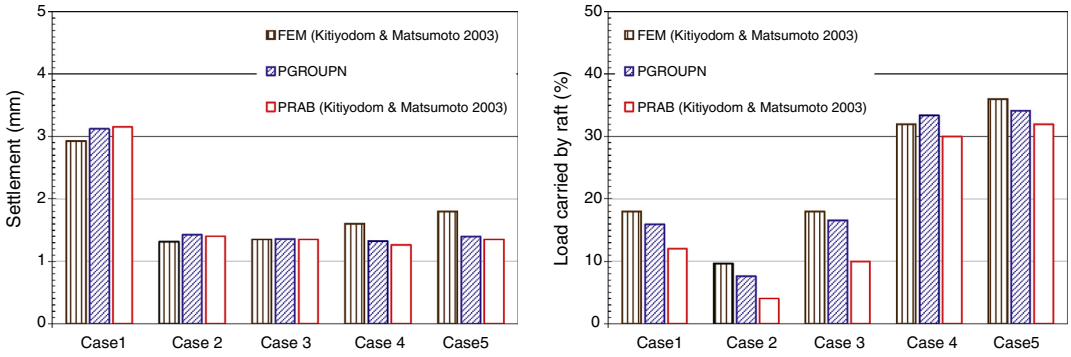

Fig. 5. (a) Settlement of piled raft and (b) load percentage carried by raft.

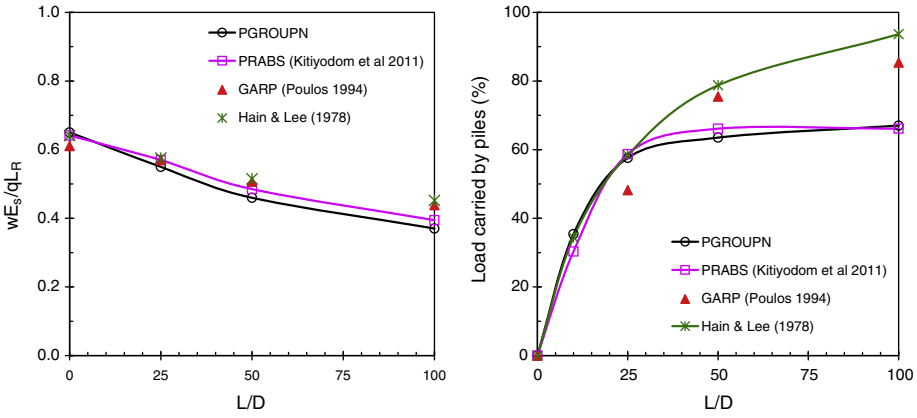

Fig. 6. (a) Normalised settlement of piled raft and (b) load percentage carried by piles.

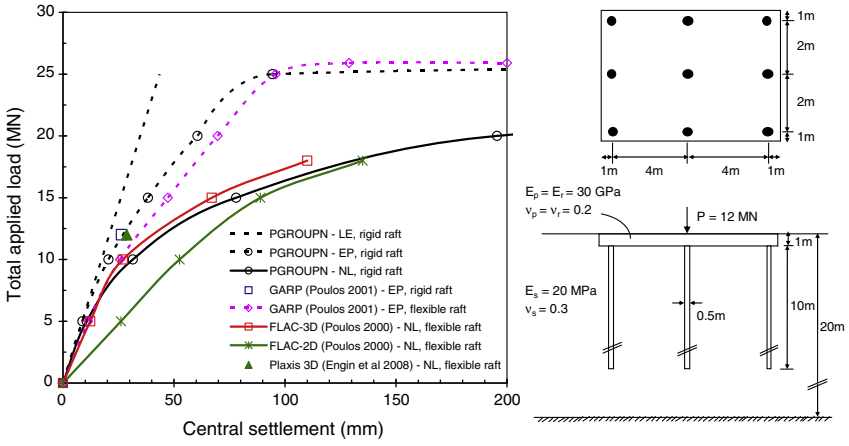

Fig. 7. Load–settlement response and piled raft analysed.

for both the piles and the raft). A variety of published numerical solutions is considered, as follows:

(1) GARP by Poulos [25,27] using an elastic-perfectly plastic soil model (EP) and assuming either a rigid (i.e. a raft thickness $t_r = 1$ m giving $K_{rs} = 6.1$ from Eq. (6)) or flexible raft (i.e. $t_r = 0.5$ m giving $K_{rs} = 0.8$).
(2) FLAC-3D finite difference analysis (using the flexible raft with $t_r = 0.5$ m) as carried out by Poulos [26] using solid elements to model the piles, the raft, and the soil, with the latter being modelled as a Mohr–Coulomb material.
(3) FLAC-2D finite difference analysis (using the flexible raft with $t_r = 0.5$ m) as performed by Poulos [26] using a Mohr–Coulomb model for the soil and assuming plane-strain conditions, with the piles and loads "smeared" over a 6 m width.
(4) Plaxis 3D finite element analysis (using the flexible raft with $t_r = 0.5$ m) as carried out by Engin et al. [9] using the embedded pile model (i.e. a simplified model of the volume pile).

The following observations are made from the load–settlement response shown in Fig. 7:

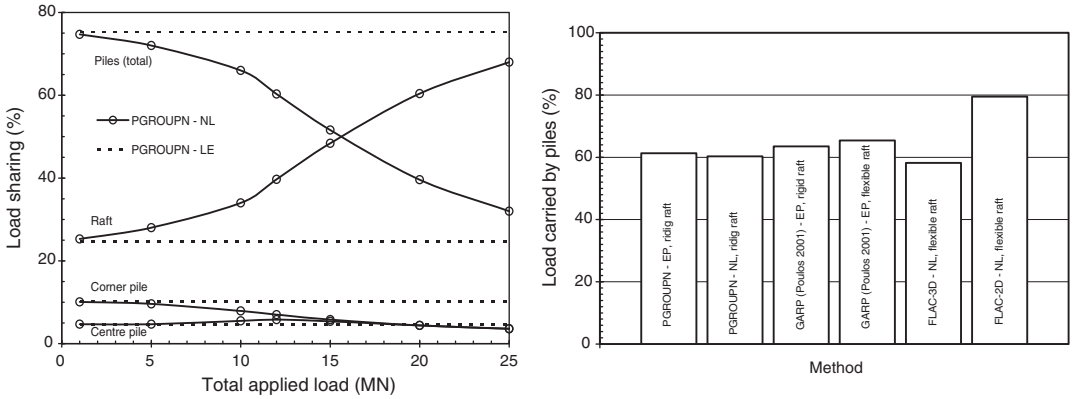

Fig. 8. (a) Load sharing between raft and piles and (b) load percentage carried by piles.

(a) As the load capacity of the piles becomes nearly fully utilised at a load of about $P = 10$ MN, the load–settlement behaviour reflects that of the raft, which is significantly less stiff than the overall pile–raft system, while the load carried by the raft starts to increase significantly (Fig. 8a); as previously observed, the fact that some of the piles (usually the stiffer piles located around the perimeter of the group) are close to their ultimate capacity is not an issue for a piled raft and is actually inevitable for an efficient design.

(b) At a typical design load $P = 12$ MN (equivalent to an overall factor of safety of 2.15 against the piled-raft ultimate capacity of 25.9 MN), PGROUPN (EP) agrees well with the corresponding settlement value obtained by GARP (EP) for the rigid raft.

(c) The load–settlement curve of PGROUPN (EP) compares favourably with that computed by GARP (EP) for the flexible raft, thereby confirming the little effect of the raft thickness on the maximum settlement.

(d) The load–settlement response of PGROUPN (NL) agrees well with that obtained by FLAC-3D (NL) for the flexible raft; PGROUPN (NL) also compares favourably with the settlement value calculated by Plaxis 3D (NL) for the flexible raft under the design load $P = 12$ MN.

(e) FLAC-2D (NL) seriously over-predicts the settlements because of the implicit assumption of plane-strain in the analysis.

The load sharing between the raft and the piles as a function of the total applied load as computed by PGROUPN is reported in Fig. 8a, showing a significant reduction of the total load carried by the piles with increasing load level because of the raft's contribution (such reduction cannot clearly be modelled by the linear elastic analysis). The values of load percentage carried by the piles under the design load $P = 12$ MN are compared in Fig. 8b, showing a generally good agreement between analyses (except for an overestimation of pile load computed by FLAC-2D).

Overall, the comparison presented in Figs. 7 and 8 shows a reasonably good agreement between the computed response from all methods other than the FLAC-2D analysis, thereby suggesting that plane-strain analyses of piled rafts must be approached with extreme caution because the results may be misleading especially for square or rectangular rafts [26]. The comparison also demonstrates the importance of considering soil nonlinearity effects in order to obtain realistic predictions of the settlement and the load sharing between the raft and the piles. Indeed, assumption of linear elastic behaviour beyond a load of about 10 MN would lead to an under-estimation of the settlement (Fig. 7) and an over-estimation of the amount of load carried by the piles (Fig. 8a), with a consequent over-design of the requirements for structural strength of the piles. As emphasised by Poulos [28], an analysis which accounts for soil nonlinearity, even though in an approximate manner, is preferable to a complex analysis in which linear soil behaviour is assumed.

3.5. Case history

The case history for the Messe-Torhaus building in Frankfurt is presented, as reported by Sommer et al. [34]. The 30-storey tall building was constructed during 1982–84 and was the first structure designed as a piled raft in Germany. The building is supported by two separate piled rafts, each with 42 bored piles with a length of 20 m and a diameter of 0.9 m. The piles under each raft are arranged in a 6×7 rectangular configuration with a centre-to-centre spacing of 2.9 m and 3.5 m along the shorter and the larger side of the raft, respectively, as indicated in Fig. 9. Each raft is 17.5 m $\times$ 24.5 m in plan, 2.5 m thick and is founded at 3 m below ground surface. During construction, the behaviour of the piled raft was carefully monitored by a geotechnical measurement programme, as described by Sommer and colleagues.

The piled raft is embedded in the Frankfurt clay which is a stiff, overconsolidated clay. In the PGROUPN analysis, it is assumed that the undrained shear strength (C_u) increases linearly with depth from 100 kPa at the foundation level to 200 kPa at the pile base, with an undrained Young's modulus derived from the correlation $E_s/C_u = 600$ and a Poisson's ratio of 0.5. It is noted that the above soil parameters are equal to those adopted in the approximate

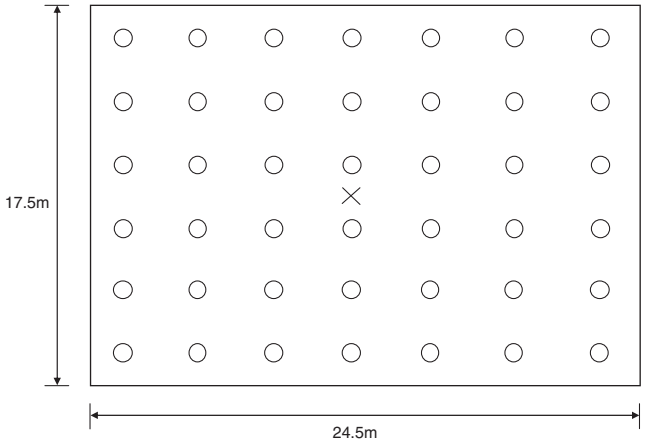

Fig. 9. Messe-Torhaus: pile arrangement.

variational approach by Chow et al. [6] so that a direct comparison between analyses may be made. For consistency with the Chow analysis, an elastic-perfectly plastic soil model has been adopted (i.e. $R_f = 0$ for both the piles and the raft) and a total load of 181 MN is assumed to centrally act on the piled raft (as only approximately 75% of the total structural load of 241 MN was applied at the time of the measurements reported herein). In addition, the following parameters have been assumed (as these were not reported by Chow and colleagues): an adhesion factor (α) of 0.7 (in order to achieve an ultimate pile load of about 7 MN, given that the measurements showed that piles were carrying at least this amount of load, as discussed by [32]), and a Young's modulus of 23.5 GPa for the piles and 34 GPa for the raft (as reported by [30]). It is noted that $K_{rs} = 2.2$ results from Eq. (6) and, hence, the PGROUPN assumption of rigid raft can be reasonably applied, as confirmed by the field measurements which showed that the raft actually behaved as rigid.

The maximum settlement of the piled raft and the proportion of load carried by the raft are reported in Fig. 10 showing a good agreement between analyses and measurements. In this case, soil nonlinearity appears to have only a relatively small effect on the computed response (at least in terms of settlement and load carried by the raft). The rather low value of the measured load carried by the raft (20%) suggests that the effect normally intended by a piled raft was not realised, thereby indicating a quite conservative design. Indeed, the contact pressures between raft and soil are scarcely larger than those due to the dead weight of the raft (i.e. about 25 MN, resulting in a load proportion of 14%), so that almost the complete load of the superstructure is carried by the piles. Thus, while the aim of reducing settlements of the foundation in comparison to a shallow foundation has been reached (resulting in a reduction of about 50%), a more efficient design could have been achieved using fewer piles of greater length. Indeed, PGROUPN shows that an identical value of settlement (i.e. 44 mm) can be attained with a significantly smaller total pile length, specifically with 25.5 m long piles in a 4×5 group configuration (at a spacing of 5.0 m and 5.5 m along the shorter and the larger side of the raft, respectively). In this case, a better ratio of the raft–pile load sharing could have been achieved (i.e. 23%) with a saving of 39% in total pile length, i.e. from 840 m for the original 6×7 group ($L = 20$ m) to 510 m for the 4×5 group ($L = 25.5$ m). Finally, it is observed that PGROUPN non-linear analyses for the 6×7 and 4×5 group configurations run in 3 and 1 min, respectively, on an ordinary computer (Intel Core i7 2.7 GHz), thereby resulting in negligible computing costs for design.

4. Design example

The hypothetical design example shown in Fig. 11 is described in order to demonstrate that, in suitable ground conditions, a significant reduction of the piling requirements can be achieved with the use of a piled raft as compared to a conventional pile foundation. Two foundation systems are evaluated:

(1) A 4×4 pile group (i.e. with no raft contribution) designed according to a traditional approach in which an overall (geotechnical) factor of safety $FS = 2$ is assumed to apply to the maximum axial force of the single pile.
(2) A piled raft (3×3 group) in which $FS = 2$ is assumed to apply to the total force acting on the whole pile–raft system.

A total force $E_k = 25$ MN is acting on the foundation and a maximum allowable settlement of 25 mm is prescribed. The analyses are carried out using PGROUPN (non-linear soil model) with the parameters indicated in Fig. 11 (the raft may be considered as fully rigid being $K_{rs} = 10.5$). The initial solution of an unpiled raft (11 m × 11 m) is discarded due to both bearing capacity and settlement requirements, given that the raft bearing capacity is equal to 54.5 MN (based on $q_u = 6C_u$) and the raft settlement results in 38 mm. Thus, a pile-group solution is considered and it is found that a group of 4×4 piles (30.5 m long) at a spacing of $3D = 3$ m is required in order to achieve $FS = 2$ on the maximum axial force (V_{max}) of the corner pile (i.e. $Q_{allowable} = 2421$ kN > $V_{max} = 2390$ kN). It is noted that the calculated pile-group settlement is equal to 14 mm, i.e. well below the allowable value of 25 mm, thereby indicating that a design optimisation may be achieved.

A piled raft solution (3×3 group with pile spacing of $4D = 4$ m and pile length of 20 m) is then evaluated following the methodology outlined in the ISSMGE CPRF Guideline [14]. According to the guideline, a sufficient safety against failure of the overall pile–raft system is achieved by fulfilling the following in equation:

$$E_d \leqslant R_d \rightarrow E_k \cdot \gamma_F \leqslant \frac{R_{tot,k}}{\gamma_R} \rightarrow E_k \cdot \gamma_F \cdot \gamma_R \leqslant R_{tot,k} \tag{7}$$

where E_k is the characteristic total force acting on the CPRF, γ_F and γ_R are the partial safety factors on actions and resistance, respectively, and the characteristic value of the total resistance $R_{tot,k}$ has to be derived from the load–settlement response of the CPRF and is equal to the load at which the increase of the settlement becomes increasingly superproportional, as determined from a "numerical" load test. In order to allow a direct comparison with the above pile-group solution, it is assumed that an overall $FS = 2$ applies to the force E_k (this assumption is equivalent to consider a value of $\gamma_F \cdot \gamma_R = 2$). This implies that Eq. (7) is fulfilled by proving that $R_{tot,k} \geqslant 2E_k = 2 \cdot 25 = 50$ MN. Thus, using PGROUPN, a numerical load test is performed to generate the typical load–settlement curve (i.e. the CPRF overall resistance), as illustrated in Fig. 11. From this figure, it can be seen that, up to the loading of 50 MN, the increase of the settlement is not yet superproportional (i.e. $R_{tot,k} > 50$ MN), implying that no significant failure of the CPRF has occurred. Thus,

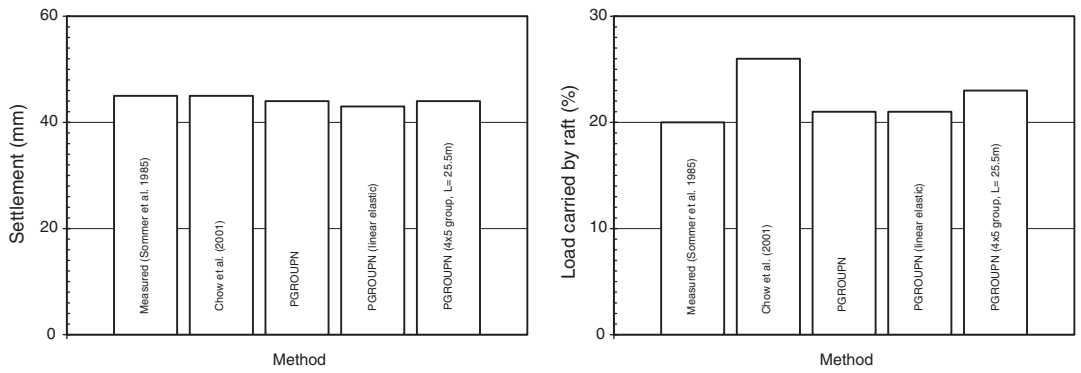

Fig. 10. (a) Settlement of piled raft and (b) load percentage carried by raft.

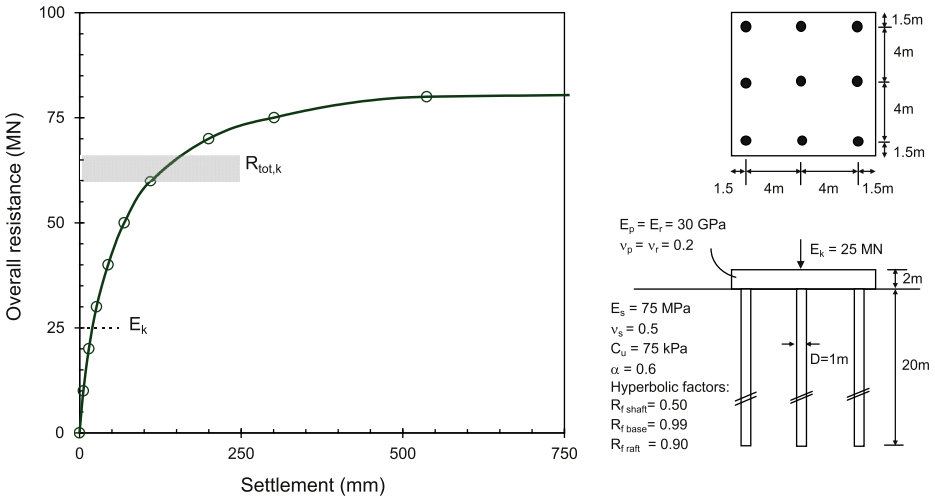

Fig. 11. Load–settlement response and piled raft analysed.

the ultimate bearing capacity (ULS) of the piled raft is proved. It is noted that the maximum pile axial load is equal to $V_{max} = 2210$ kN, which would give $FS = 1.5$ (being the ultimate pile capacity $Q_{ult} = 3358$ kN); however, in contrast to conventional pile foundations, the proof of the bearing capacity for single piles is unnecessary because this proof is inconsistent with the concept of piled rafts. Within the same numerical load test, proof of the serviceability limit state (SLS) for the piled raft can be performed and, under the total load of 25 MN, a settlement of 20 mm is calculated, i.e. below the allowable value of 25 mm. It is found that at this load level the raft carries 39% of the total load.

Finally, it should be emphasised that the piled raft solution leads to a significant reduction in the required number and length (L) of the piles as compared to the conventional pile group, resulting in a saving of 63% in total pile length, i.e. from 488 m for the 4×4 pile group ($L = 30.5$ m) to 180 m for the 3×3 piled raft ($L = 20$ m).

5. Conclusions

The paper has described a practical analysis method, based on a 3D complete BEM solution and implemented in the code PGROUPN, for determining the non-linear response of piled rafts. The method has been successfully validated against alternative numerical analyses and field measurements. It has been shown that the concept of piled raft, generally adopted for "large" flexible piled rafts, can also be applied effectively to "small" rigid piled rafts (and to any larger piled raft in which the assumption of rigid raft is valid), making PGROUPN ideally suitable to a wide range of foundations such as bridges, viaducts, wind turbines and ordinary buildings (where use of 3D FEM or FDM analyses would be uneconomical). In such cases, if the raft can be founded in reasonable competent ground (which can provide reliable long-term resistance), then the extra raft component of capacity can be used to significantly reduce the piling requirements which are necessary to achieve the design criteria (e.g. ultimate bearing capacity, settlement).

Given the relatively high load level at which the piles operate within a pile–raft system, the influence of soil nonlinearity can be significant, and ignoring this aspect can lead to inaccurate predictions of the deformations and the load sharing between the raft and the piles. Consideration of soil nonlinearity would also be required if PGROUPN is used to perform a numerical load test following the methodology outlined in the ISSMGE CPRF Guideline. Due to the negligible costs (both in terms of data preparation and computer execution times), a large number of cases can be analysed efficiently, enabling parametric studies to be readily performed, thus offering the prospect of more effective design techniques and worthwhile savings in construction costs.

Conflict of interest

There is no conflict of interest in this paper.

References

[1] Basile F. Non-linear analysis of pile groups. Proc Inst Civ Eng, Geotech Eng 1999;137(2):105–15.
[2] Basile F. Analysis and design of pile groups. In: Bull JW, editor. Numerical analysis and modelling in geomechanics. Spon Press; 2003. p. 278–315.
[3] Bond AJ, Basile F. Repute 2.0, Software for pile design and analysis. Reference manual, Geocentrix Ltd, UK, 2012. 53p.
[4] Brinch Hansen J. A revised and extended formula for bearing capacity. Danish Geotech Inst Bull 1970;28:5–11.
[5] Butterfield R, Banerjee PK. The problem of pile group-pile cap interaction. Géotechnique 1971;21(2):135–42.
[6] Chow YK, Yong KY, Shen WY. Analysis of piled raft foundations using a variational approach. Int J Geomech 2001;1(2):129–47.
[7] Clancy P, Randolph MF. Analysis and design of piled raft foundations. Int J Numer Anal Meth Geomech 1993;17:849–69.
[8] Duncan JM, Chang CY. Non-linear analysis of stress and strain in soils. J Soil Mech Found Div, ASCE 1970;96(SM5):1629–53.
[9] Engin HK, Septanika EG, Brinkgreve RBJ. Estimation of pile group behavior using embedded piles. In: Proc 12th IACMAG int conf, Goa, India, 2008. p. 3231–38.
[10] Fraser RA, Wardle LJ. Numerical analysis of rectangular rafts on layered foundations. Geotechnique 1976;26(4):613–30.
[11] Hain SJ, Lee IK. The analysis of flexible raft–pile systems. Geotechnique 1978;28(1):65–83.
[12] Horikoshi K, Randolph MF. On the definition of raft–soil stiffness ratio. Géotechnique 1997;47(5):1055–61.
[13] Jeong S, Cho J. Proposed nonlinear 3-D analytical method for piled raft foundations. Comput Geotech 2014;59:112–26.
[14] Katzenbach R, Choudhury D. ISSMGE combined pile–raft foundation (CPRF) guideline. Darmstadt, Germany: Technische Universität Darmstadt; 2013. 23p.
[15] Kitiyodom P, Matsumoto T. A simplified analysis method for piled raft foundations in non-homogeneous soils. Int J Numer Anal Meth Geomech 2003;27:85–109.
[16] Kitiyodom P, Matsumoto T, Sonoda R. Approximate numerical analysis of a large piled raft foundation. Soil Found 2011;51(1):1–10.
[17] Kuwabara F. An elastic analysis for piled raft foundations in homogeneous soil. Soil Found 1989;29(1):82–92.
[18] Lee JH, Kim Y, Jeong S. Three-dimensional analysis of bearing behavior of piled raft on soft clay. Comput Geotech 2010;37(1–2):103–14.
[19] Mandolini A, Russo G, Viggiani C. Pile foundations: experimental investigations, analysis and design. In: Proc 16th int conf soil mechanics geotech eng, Osaka, vol. 1, 2005. p. 177–213.
[20] Mindlin RD. Force at a point in the interior of a semi-infinite solid. Physics 1936;7:195–202.

[21] Moyes P, Poulos HG, Small JC, Badelow F. Piled raft design process for a high-rise building on the Gold Coast, Australia. In: Proc. 6th int conf on tall buildings, 2005. p. 241–9.
[22] Nguyen DDC, Jo SB, Kim DS. Design method of piled-raft foundations under vertical load considering interaction effects. Comput Geotech 2013;47:16–27.
[23] O'Brien AS, Burland JB, Chapman T. Rafts and piled rafts. ICE manual of geotechnical engineering, vol. 2. UK: Institution of Civil Engineers; 2012. p. 853–86 [Chapter 56].
[24] Poulos HG. Pile behaviour – Theory and application. 29th Rankine Lecture, Géotechnique 1989;39(3):365–415.
[25] Poulos HG. An approximate numerical analysis of pile–raft interaction. Int J Numer Anal Meth Geomech 1994;18:73–92.
[26] Poulos HG. Pile-raft interaction – alternative methods of analysis. In: Smith DW, Carter JP, editors. Developments in theoretical geomechanics. Rotterdam: Balkema; 2000. p. 445–63.
[27] Poulos HG. Piled-raft foundation: design and applications. Géotechnique 2001;51(2):95–113.
[28] Poulos HG. Significance of interaction and non-linearity in piled raft foundation design. In: Orense, Chouw, Pender, editors. Soil-foundation-structure interaction, 2010. p. 187–92.
[29] Randolph MF. Science and empiricism in pile foundation design. 43rd Rankine Lecture, Géotechnique 2003;53(10):847–75.
[30] Reul O, Randolph MF. Piled rafts in overconsolidated clay: comparison of in-situ measurements and numerical analyses. Géotechnique 2003;53(3):301–15.
[31] Shen WY, Chow YK, Yong KY. A variational approach for the analysis of pile group-pile cap interaction. Géotechnique 2000;50(4):349–57.
[32] Small JC, Poulos HG. Non-linear analysis of piled raft foundations. In: Contemporary issues in deep foundations, GSP 158, ASCE, 2007. p. 1–9.
[33] Small JC, Zhang HH. Piled raft foundations subjected to general loadings. In: Smith, Carter, editors. Proc booker memorial symposium, in developments in theoretical geomechanics. Rotterdam: Balkema; 2000. p. 431–45.
[34] Sommer H, Wittmann P, Ripper P. Piled raft foundation of a tall building in Frankfurt clay. In: Proc 11th int conf soil mechanics foundation engineering, San Francisco, 1985. p. 2253–57.
[35] Ta LD, Small JC. Analysis of piled raft systems in layered soils. Int J Numer Anal Meth Geomech 1996;20:57–72.
[36] Viggiani C, Mandolini A, Russo G. Piles and pile foundations. Spon Press; 2012. 278p.